GAS TEMPERATURE DETERMINATION OF NON-THERMAL ATMOSPHERIC PLASMAS FROM THE COLLISIONAL BROADENING OF ARGON ATOMIC EMISSION LINES

A. Rodero[1] and M.C. García[1,*]

[1]*Grupo de Física de Plasmas: Diagnosis, Modelos y Aplicaciones (FQM-136)*

Edificio A. Einstein (C-2), Campus de Rabanales. Universidad de Córdoba, 14071 Córdoba, Spain

[*]*Author for correspondence, e-mail: fa1gamam@uco.es*

Abstract

In this work we propose a new method allowing gas temperature determination in argon non-thermal plasma jets, based on the measurement of the collisional broadening of different argon atomic lines corresponding to transitions into both resonance levels s_2 and s_4 of the $3p^5 4s$ configuration. The method was developed for fourteen lines: Ar I 978.45, 935.42, 922.45, 852.14, 840.82, 826.45, 750.39 (corresponding to transitions falling to level s_2) and 965.77, 842.46, 810.37, 800.62, 751.46, 738.40, 727.29 nm (corresponding to transitions falling to level s_4). A carefully study of the relative importance of all broadening mechanisms to the whole profile for these lines, under a broad range of experimental conditions, revealed that for electron densities and gas temperature lower than 10^{15} cm^{-3} and 2000 K, the Stark and Doppler broadenings can be neglected in the method, but the van der Waals contribution should not be ever discarded for gas temperature determination. The gas temperature of a microwave non-thermal plasma jet was determined using nine of these lines. Results were consistent with each other, and with those obtained from the rotational temperature derived from OH ro-vibrational band. Also,

the influence of the air entrance on the collisional broadening of the lines has been studied and the way the method should be modified to include this effect is indicated.

Keywords: Plasma spectroscopy, non-thermal plasmas, gas temperature, collisional broadening, atomic emission spectroscopy.

1. Introduction.

In the two last decades, the development of cold plasma sources operating in the open atmosphere has noteworthy grown. Besides of simplicity of handing conferred by the atmospheric pressure condition, their low power consumption and their capacity to induce physical and chemical processes at relatively low gas temperatures are properties making them very attractive from an applied point of view. It is well known that the reactivity of these plasmas comes from their high energy electrons, while the ions and neutral species retain a *gas temperature* (or heavy particles temperature) T_g relatively cold.

In technological applications, such as those related to plasma surface treatments (thin film deposition, sterilization, surface functionalization…) or plasma treatment of liquids, a reliable determination of the gas temperature in the plasma could be crucial. But, to control this plasma characteristic parameter becomes particularly relevant when applying cold plasma technology directly on living human (and animal) cells, tissues and organs. In the last few years, a large variety of cold atmospheric plasma (CAP) sources for therapeutic uses in the medicine area [1-5] have been designed.

Optical Emission Spectroscopy (OES) techniques based on the analysis of molecular emission spectra are commonly used for gas temperature determination of plasmas sustained at atmospheric pressure. The rotational temperature derived from them is considered as a good estimation of the kinetic temperature of the plasma heavy particles due to the strong coupling between translational and rotational energy states under these high pressure conditions [6-13]. Nevertheless, the use of molecular emission spectroscopy is not always easy for gas temperature measurement in plasmas [14-17]. Overlapping of bands, rotational population distribution of levels having a non-Boltzmann nature, wake emission of rotational bands, among others, can make difficult to obtain reliable values of

gas temperature. Also, some of these techniques have been shown to be poor sensitive for gas temperature determination in CAP conditions, near the room temperature [18].

Alternative OES methods for gas temperature determination in cold plasmas are then needed, and those based on the analysis of atomic lines profiles could be a good option. In this way, the *van der Waals* broadening of some argon atomic lines (broadening related to the plasma gas temperature, as we will show later) have been used for this purpose [19-22]. This technique is based on detection of argon atomic lines (Ar I 425.94, 522.13, 549.61 and 603.21 nm) not having resonance broadening (also related to T_g), but requires the use of additional techniques for simultaneous electron density determination, as these lines have a non negligible *Stark* broadening for electron densities above 10^{14} cm^{-3} which needs to be determined. Yubero et al. in [23] have proposed a way to circumvent this dependence on electron density considering pairs of these lines.

Recently Pipa et al. [18] have proposed a new method for gas temperature determination from the resonance broadening of some argon emission lines (Ar I 750.39, 826.45, 840.82, 852.14, 922.45 and 978.45 nm), corresponding to transitions into the resonance level s_2 (Paschen notations) of the $3p^5 4s$ configuration. This method sustains on three premises: (i) these lines have a strong resonance broadening related to the gas temperature; (ii) they have a negligible Stark broadening for electron densities under 10^{15} cm^{-3} (so, additional measurements of electron densities are not needed); and (iii) according to the authors's claim (supported on some references they cited), these lines have a *van der Waals* broadening that can be also neglected.

In the present work, we propose a new method allowing gas temperature determination in argon non-thermal plasma jets with T_g < 2000 K (so also in cold plasma jets), based on the measurement of the collisional broadening of different argon atomic lines, all of them corresponding to transitions into both resonance levels s_2 and s_4 of the

$3p^5 4s$ configuration. We developed this method for fourteen different lines (so actually, we present fourteen different tools): Ar I 978.45, 935.42, 922.45, 852.14, 840.82, 826.45, 750.39 (corresponding to transitions falling to level s_2) and 965.77, 842.46, 810.37, 800.62, 751.46, 738.40, 727.29 nm (corresponding to transitions falling to level s_4). As a previous step, we have studied the relative importance of the different mechanisms causing the broadening of each of these lines emitted by the plasma, i.e. the relative contribution of the different broadening mechanisms to the whole line profile. Particularly, the relative importance of resonance and van der Waals broadenings have been determined in order to elucidate whether or not the van der Waals contribution could be neglected under some specific experimental conditions of electron density and gas temperature. We will demonstrate that this contribution should not be discarded under any T_g condition. Furthermore, when using these lines, the van der Waals contribution to the whole broadening could be especially critical in the determination of the gas temperature of CAPs (with T_g under 350 K).

The new methods we propose in this work have been applied to gas temperature determination of an argon microwave jet open to the air. The values of the temperatures obtained using them, have been compared to the rotational temperatures derived from the OH ro-vibrational bands for validation.

Cold argon plasma jets for both technological and medical uses are very common, as operation in a noble gas atmosphere yields the advantage of accurate control of (biologically or not) active species generation by admixture of oxygen or nitrogen as well as water vapor. Anyway, also similar methods using different atomic lines (helium, oxygen,…) could be also developed for plasmas operating in other gases.

2. Line broadening mechanisms

In plasmas generated at atmospheric pressure with no presence of magnetic fields, atoms emission is generally broadened due to different effects. The combination of Doppler and pressure broadenings (encompassing Stark, van der Waals and resonance broadenings), gives rise to an emitted line profile, that eventually can experiment additional broadening mechanisms (instrumental and self-absorption broadenings) during the detection process by the optical system. As a result, the line profile detected can be reasonably well fitted to a Voigt function in many cases.

Next, we will briefly describe these broadening mechanisms in order to review the plasma or optical system characteristic parameters determining each of them.

2.1 Collisional broadenings

Emitting atoms suffer frequent collisions with other atoms and ions in the plasma, which produces distortion of their energy levels. This is a mechanism leading to the so called *collisional or pressure broadening* of the emission lines. Depending on the nature of disturbing particles, there are different types of collisional broadenings: *van der Waals*, *resonance* and *Stark* broadenings.

The *van der Waals (VDW) broadening* is due to dipole moment induced by neutral atom perturbers in the instantaneous oscillating electric field of the excited emitter atom and generates line profiles with a Lorentzian shape with a FWHM W_W that, according to the Lindholm-Foley theory [24], is given (in nm) by

$$W_W = 8.18 \cdot 10^{-12} \lambda^2 \left(\alpha \left\langle \overline{R^2} \right\rangle \right)^{2/5} \left(T_g / \mu \right)^{3/10} N \tag{1}$$

where

$$\left\langle \overline{R^2} \right\rangle = \left\langle \overline{R_U^2} \right\rangle - \left\langle \overline{R_L^2} \right\rangle \tag{2}$$

is the difference of the squares of coordinate vectors (in a_0 units) of the upper and lower level of the transition, λ the wavelength of the observed line in nm, α is the polarizability of perturbers interacting with the excited radiator in cm^3, T_g is the temperature of the emitters (coincident with the gas temperature) in K, μ is the atom-perturber reduced mass in a.m.u., and N is the density of perturbers in cm^{-3}.

In the Coulomb approximation, $\left\langle \overline{R_i^2} \right\rangle$ for a specific line can be calculated from:

$$\left\langle \overline{R_i^2} \right\rangle = \frac{1}{2} n_i^{*2} \left[5n_i^{*2} + 1 - 3l_i(l_i+1) \right] \tag{3}$$

being n_i^* the effective quantum number, which can be obtained from the hydrogen approximation as

$$n_i^{*2} = \frac{E_H}{E_P - E_i} \tag{4}$$

where E_P is the ionization level of the radiating atom, E_H is the Rydberg constant and E_i is the excitation energy of the upper or lower level of the transition corresponding to the line.

Considering the ideal gas equation $N = P/K_B T_g$, the expression for the FWHM due to van der Waals broadening can be written as,

$$W_W(T_g) = \frac{C_W}{T_g^{0.7}} (\text{nm}) \tag{5}$$

with C_W being determined by the type of gas in the discharge and the nature of the atom emitters:

$$C_W = \frac{8.18 \cdot 10^{-19} \lambda^2 \left(\alpha \left\langle \overline{R^2} \right\rangle \right)^{2/5} P}{k_B \mu^{3/10}} \qquad (\mathrm{nm} \cdot \mathrm{K}^{7/10}) \tag{6}$$

For an argon plasma at atmospheric pressure, when considering the van der Waals broadening of argon atomic lines ($\mu = 19.97$ and $\alpha = 16.54 \cdot 10^{-25}$ cm^3), C_W can be written as

$$C_W = 7.5 \cdot 10^{-7} \lambda^2 \left(\left\langle \overline{R^2} \right\rangle \right)^{2/5} (\mathrm{nm} \cdot K^{7/10}) \tag{7}$$

In short, the van der Waals broadening is also characteristic for every atomic line emitted and it is related to the gas temperature in the plasma.

The *resonance broadening* of spectral lines is due to dipole-dipole interactions of the emitter with ground-state atoms of the same element. This broadening mechanism originates a Lorentzian shaped profile with a FWHM W_R given (in Å) by [25-26]:

$$W_R \approx 8.6 \times 10^{-30} \left(\frac{g_i}{g_k} \right)^{1/2} \lambda^2 \lambda_r f_r N \tag{8}$$

where λ is the wavelength of the observed line (in Å); f_r and λ_r are the oscillator strength and wavelength (in Å) of the line; g_k and g_i are the statistical weights of its upper and lower levels and N is density of perturber atoms (ground state atoms in cm^{-3}).

Considering $N \approx P/K_B T_g$, the expression for the FWHM can be written as

$$W_R(T_g) = \frac{C_R}{T_g} (\mathrm{nm}) \tag{9}$$

being the value of C_R characteristic for every spectral line.

Resonance broadening is then related to the gas temperature and leads to a Lorentzian shaped profile [27]. Let us remark again that this broadening is not affecting every single spectral line in the spectrum, but only those corresponding to transitions with upper and lower levels having electric dipole transitions to the ground state.

The *Stark broadening* results from Coulomb interactions between the emitter atom and surrounding charged particles, perturbing the electric field it experiences. Both ions and electrons induce Stark broadening, but in non-thermal plasmas, electrons are responsible for the major part of it because of their higher relative velocities. The Stark broadening depends on both electron density and temperature (n_e, T_e).

For non-hydrogenic atoms (such as argon ones), the line broadening due to the Stark effect of electrons in impact approximations results in a Lorentzian shaped profile [27] with a FWHM W_S having a dependence on the electron density that can be expressed as:

$$W_S(T_e, n_e) \approx w_e(T_e)\frac{n_e}{10^{16}} \tag{10}$$

where n_e is given in cm^{-3} and $w_e(T_e)$ is Stark parameter for a density of 10^{16} cm^{-3}, which has been calculated by several authors for different atomic lines in plasmas under different conditions [28-31].

The total collisional broadening result from the convolution of these three mechanisms, giving rise to a Lorentzian profile with a FWHM W_L (or W_C) given by:

$$W_L(T_g, n_e, T_e) = W_C(T_g, n_e, T_e) = W_W(T_g) + W_R(T_g) + W_S(n_e, T_e) \tag{11}$$

As already mentioned, in this work, we propose several (fourteen) new tools based on the measurement of the collisional broadening of fourteen argon atomic lines corresponding to all transitions into the resonance levels s_2 and s_4 of the $3p^5 4s$ configuration (see Table I).

The contribution of each specific mechanism to the total collisional broadening has been studied in order to evaluate the most important effects, and whether or not any of them could be neglected. In order to determine these contributions, constants C_W and C_R in Eqs. (5) and (9) have been calculated for each one of the fourteen lines (see Table II). We have used data from NIST atomic data base [32] to calculate $\left\langle \overline{R^2} \right\rangle$ in eq. (7), for every line. Also, data from NIST for the resonant lines Ar I 104.82 nm (f_r = 0.25, g_i = 1, g_i = 3) and Ar I 106.67 nm (f_r = 0.0609, g_i = 1, g_i = 3), were used to evaluate C_R from Eq. (9), for lines corresponding to transitions to s_2 and s_4 level, respectively.

The Stark parameters w_e of these lines corresponding to an electron temperature of 10,000 K are also collected in Table II for most of lines (although for some of them, no data have been found). The dependence of these parameters on T_e is weak, so conclusions about the contribution of these broadenings also apply to temperatures of similar order.

Lines chosen in this work are affected by a relatively high resonance broadening. The oscillator strength f_r for argon resonance radiation from the s_4 level is about four times lower than that from the s_2 level, so, according to Eq. 9, the resonance broadening of lines corresponding to transitions $p \rightarrow s_4$ is expected to be significantly lower. So, we will consider two groups of lines: (i) to the first one belong the lines corresponding to transitions $s_4 - p$; for these lines resonance and van der Waals broadening are in the same order of magnitude; (ii) in the second one are lines corresponding to transitions $s_2 - p$, for which the resonance broadening is notably higher. In our reasoning below, line Ar I 750.39

nm has been used as representative of the first group, and line Ar I 842.46 nm as representative of the second one.

Figures 1 (a) and (b) show the contribution of each collisional mechanism to the total collisional broadening FWHM W_C, as a function of T_g in the case of resonance and van der Waals broadenings, and as a function of n_e in the case of the Stark broadening for a typical value of electron temperature T_e = 10,000 K.

We can observe that, in both cases, for electron densities below 10^{15} cm^{-3} the Stark broadening is much lower than other two mechanisms (resonance and van der Waals), over the whole range of low gas temperatures below 2000 K. Similar behaviors have been found for the rest of lines studied here.

This fact can be also observed from the representation of the dependence of W_C on the gas temperature, for different values of electron densities (see Figs. 2(a) and (b) for lines Ar I 750.39 nm and Ar I 842.46 nm, respectively).

Then, these dependences are almost unaffected when considering the Stark broadening contribution for electron densities below 10^{15} cm^{-3}. As a consequence, we can neglect the Stark contribution to the total collisional broadening, and W_C could be considered as only dependent on T_g:

$$W_C(T_g) \approx W_W(T_g) + W_R(T_g) = \frac{C_W}{T_g^{0.7}} + \frac{C_R}{T_g} \tag{12}$$

According to this expression, the gas temperature can be obtained from the value of W_C experimentally measured.

Pipa et al. in reference [18] considered also negligible the van der Waals contribution to the whole collisional broadening, when they were using lines of high resonance broadening corresponding to transitions $s_2 - p$ for gas temperature determination. In the

present work, we will demonstrate that under all experimental conditions, the van der Waals contribution does affect the collisional broadening of all these Ar I lines falling to the resonance levels of the $3p^5 4s$ configuration, so that this contribution must be always considered. Figures 3(a) and (b) show this fact by comparing W_C values obtained with and without taking into account the van der Waals contribution for lines Ar I 750.39 nm and ArI 842.46 nm, respectively.

2.2 Doppler broadening

Lines emitted by the plasma are also influenced by the so-called Doppler broadening due to the motion of emitter atoms with respect to the detector, with a continuous velocity distribution depending on their temperature. This contribution a Gaussian-shaped line profile with a full-width at half-maximum, FWHM, W_D given (in nm) by

$$W_D(T_g) = 7.16 \cdot 10^{-7} \lambda \sqrt{T_g / M} \tag{13}$$

where T_g and M are the temperature (in K) and mass of the radiating atom (in a.m.u.). This broadening is then specific for every atomic line and is related to the gas temperature of the plasma.

The joint contribution of collisional and Doppler broadenings gives rise to a Voigt profile resulting from the convolution of a Lorentzian with and a Gaussian profile. The FWHM of this Voigt profile W_V can be approximated by the following expression:

$$W_V \approx \frac{W_L}{2} + \sqrt{\left(\frac{W_L}{2}\right)^2 + W_G^2} \tag{14}$$

In this way, as $W_L = W_C$ and $W_G = W_D$, Eq. (14) can be written as:

$$W_V \approx \frac{W_C}{2} + \sqrt{\left(\frac{W_C}{2}\right)^2 + W_D^2} \tag{15}$$

On the other hand, Figs. 4(a) and (b) compare the FWHM of the total Voigt profile considering and not considering the Doppler contribution, for lines Ar I 750.39 nm and ArI 842.46 nm, respectively.

As it can be observed, the Doppler contribution is only important for high values of T_g (T_g > 2000 K), being negligible for lower values. In the case of lines corresponding to transitions $s_2 - p$ (represented by the line Ar I 750.39 nm), this fact is even truer because the Doppler contribution is relatively smaller. Similar behaviors have been found for the rest of lines analyzed here in this work.

So, we can conclude that in cold plasmas, both Stark and Doppler contributions to the whole broadening for these argon lines can be neglected, and consider their emissions are Lorentzian shaped with a FWHM equal to W_C given by Eq. (12).

2.3 Instrumental broadening

Lines emitted by the plasma experiment an additional broadening when detected with the optical system. If a spectrometer is used for detection of light emitted by plasma, this *instrumental broadening* is determined by its dispersion and the slits widths. When entrance and exit slits of equal width are used, the instrumental function of spectrometer has a triangular shape that is well approximated by a Gaussian profile with a FWHM W_I given by

$$W_I = D(\lambda) l_S \tag{16}$$

where l_s is the slit width and $D(\lambda)$the dispersion of spectrometer, which depends on wavelength.

In a Czerny-Turner type spectrometer, this dispersion is given by:

$$D(\lambda) = \frac{d}{F}\left[\cos\frac{\varepsilon}{2}\sqrt{1-\left(\frac{\lambda}{2d\cos\frac{\varepsilon}{2}}\right)^2}+\frac{\lambda}{2d\cos\frac{\varepsilon}{2}}sen\frac{\varepsilon}{2}\right] \quad (17)$$

where F is the focal length of the spectrometer, d is the separation between grooves of the diffraction grating and ε is an characteristic angle that depends on the separation between mirrors and between them and the grating.

In this approximation, the resulting profile of non self-absorbed lines detected can be assumed as a Voigt function, convolution of instrumental function (Gaussian) with the collisional profile (Lorentzian). The FWHM of this Voigt shaped profile is given by an expression similar to Eq. (14):

$$W_V = \frac{W_C}{2}+\sqrt{\left(\frac{W_C}{2}\right)^2+W_I^2} \quad (18)$$

as $W_L = W_C$ and $W_G = W_I$.

2.4 Other broadening mechanisms

The light emitted by the plasma could also suffer from some self-absorption as it propagates within it. This effect that affects in varying extent the different spectral lines,

and is strongly dependent on plasma experimental conditions (size, species densities), could result in an additional broadening of the detected line. This broadening is difficult to quantify and that is the reason why atomic lines unaffected by self-absorption need to be considered when using them for plasma diagnosis from the study of their profiles.

Finally, the finite lifetime of the excited levels give rise to the *natural broadening*, which is typically very small (~ 0.00001nm) and can be neglected in the case of atmospheric pressure plasma spectroscopy.

3. Gas temperature determination method

In this work we propose several methods (corresponding to fourteen spectral lines) for gas temperature determination based on the use of the relationship between the FWHM of their collisional broadening and T_g, given by Eq. (12). For each specific case, this broadening can be obtained from the experimentally measured profile of the (no self-absorbed) Ar I line, which can be approximated by Voigt shaped profile with a FWHM given by Eq. (18). From this equation, the collisional broadening can be derived and expressed as

$$W_C = W_V - \frac{W_I^2}{W_V} \tag{19}$$

By measuring W_V and knowing the value of the instrumental broadening as a function of the wavelength from Eq. (16), W_C can be derived. Finally, the gas temperature can be determined using Eq. (12) and constants in Table II.

Figures 5(a) and (b) represent the relationship T_g (W_C) for lines Ar I 750.39 nm and Ar I 842.46 nm. Similar dependences T_g (W_C) for the rest of lines checked in this work were found (see Fig. 6).

The error in T_g determination of this method is given by the accuracy of the W_C measurement. Figs. 5(a) and (b) also show the error in gas temperature derived from the method for a typical experimental error $\Delta W_C \sim 0.001$nm,. The highest errors in T_g correspond to the zone of high values of gas temperature, reducing this error at lower T_g values. So, the method is especially useful in the determination of the gas temperature of cold plasmas (with $T_g < 350$ K).

From Eq. (12) we cannot get a mathematical dependence $T_g(W_C)$. In order to obtain such an analytical dependence allowing a straightforward determination of the gas temperature from W_C, curves in Fig. 6 have been fitted to an exponential function

$$T_g(W_C) = A_0 + A_1 \exp\left(-\frac{W_C}{t_1}\right) + A_2 \exp\left(-\frac{W_C}{t_2}\right) \tag{20}$$

These fitting give a very good approximation ($r^2 > 0.999$) in the gas temperature range between 275 and 5000 K (see Figs. 5(a) and (b)).

The analytical functions derived from these fits, for the fourteen argon lines considered, are shown in Table III.

4. Measuring the gas temperature of a microwave sustained plasma at atmospheric pressure.

We have finally applied the method using nine of Ar I lines of Table I, to the determination of the gas temperature in different regions of a microwave induced plasma sustained at atmospheric pressure. We have compared these values with those obtained from simulations of OH (A-X) ro-vibrational band, in order to validation.

4.1 Experimental set-up

Figure 7 shows a schematic of the discharge apparatus and OES system. A *surfatron* device [33] was used to couple the energy coming from a microwave (2.45 GHz) generator (with a maximum stationary power of 200 W in continuous-wave mode) to the support gas (argon with a purity ≥ 99.995 %) within a quartz reactor tube of 1.5 and 4 mm of inner and outer diameter, respectively, opened to the air as shown in Fig. 7. Surfatron was originally designed to generate cylindrical plasma columns inside straight dielectric tubes, sustained by an azimuthally symmetric TM_{00} surface wave mode. Nevertheless, in our experiments a T-shaped tube with a closed end (see Fig. 7) was employed in order to allow the plasma column go down through the vertical part of the tube. This configuration is very useful when the plasma is used for treatment of liquid samples.

In this work, the microwave power was set at 150 W and the argon flow rate was adjusted to700 sccm with the help of a calibrated mass flow controller. By means of a system of movable stubs, impedance matching was performed until the best energy coupling was achieved, making the power reflected back to the generator (P_r) negligible (< 5%).

Figure 7 also depicts schematically the experimental setup used to acquire OES measurements. Light emission from the plasma was analyzed by using a 1 m focal length Czerny-Turner type spectrometer, equipped with a 1200 grooves/mm holographic grating and a photomultiplier (spectral output interval of 300-900 mm) as a detector. The light emitted at four different axial positions of the vertical part of the plasma column (y = 6, 16, 26, 30 mm, considering y = 0 the center of horizontal tube) was side-on collected and focussed at 1:1 onto an optical fiber using an achromatic lens.

In this work, we did not use the fourteen lines for gas tempertaure determination but only nine of them. Lines Ar I 751.46 nm and 727.29 nm, overlapped to Ar I 751.04 nm and

727.06 nm, respectively, were not used (actually, they led to underestimated values of T_g that we are not going to show). Lines Ar I 978.45 nm, 965.77 nm and 935.42 nm could not be detected in our experiments.

OH ro-vibrational band (3060 Å system, A-X) was also recorded. Aditionally, the hydrogen Balmer series line H_β (at 486.13 nm) was measured in order to evaluate the order of magnitude for the electron density of this plasma [34]. The values of electron density obtained ranged between 1.2 and 3.7 10^{14} cm^{-3}, being lower 10^{15} cm^{-3}. So, on the basis of already explained considerations, the Stark mechanism broadening could be neglected. Both, H and OH species resulted from the dissociation water were present as impurity in the feed gas.

The instrumental function of the spectrometer for the wavelengths corresponding to the different measured lines was calcuted by using Eq. (17) with F = 1 m, d = 0.8 μm and ε = 0.235. The values of FWHM of instrumental funtion for these wavelengths are shown in Table IV for a slit widht of 77 μm.

In order to validate these theoretical values of W_I, the instrumental function of the spectrometer was experimentally determined for λ = 632.8 nm by using the line Ne I emitted by a helium-neon laser in this wavelength. In this way, an instrumental broadening W_I = 0.062 nm was measured when using slit widths of 77 μm. The theoretical value obtained from Eq. (17) was W_I = 0.0619 nm, that confirmed the goodness of the theoretical determination of W_I from it.

Finally, measurements of the light absorption have shown that the plasma studied can be considered as optically thin in the direction of observation chosen (transversally) for the Ar I lines detected.

4.2 Results

4.2.1 Gas temperatures from argon lines

Emission spectra from four positions of the plasma column y = 6, 16, 26 and 30 nm were taken. Figure 8 shows a typical full spectrum recorded from light emitted by the plasma in the wavelength range from 300 to 900 nm.

For every line, the spectrum was recorded several times in order to evaluate the reproducibility of the method and the experimental error in FWHM determination. For each line, dispersion in FWHM measurements was less than 0.001 nm.

Figure 9 shows the averaged values of W_V measured for the nine resonance lines detected, for these four y positions.

Using Eq. (19) and the values of W_I in Table IV, we can estimate the collisional broadening W_C for all studied lines emitted, at every axial position (see Fig. 10).

The highest values of collisional broadening were obtained for the lines corresponding to transitions into the resonance level s_2. Particularly high was W_C for Ar I 922.45 nm, although it should be noted that this line felt out of the range of efficiency of the photomultiplier used in the experiments, and it was poorly detected in our experiments, having a signal-to-noise ratio notably smaller than for the rest of lines. Lines corresponding to transitions to level s_4 had a total W_C three times lower.

Finally, using the theoretical functions gathered in Table III, the values of gas temperature, at the different plasma positions, were calculated. Fig. 11 shows the values of T_g measured from different Ar I lines. Values measured at positions y = 6 and y = 16 mm, with different lines were consistent with each other, being similar within the error bar of the measurements.

However, at positions y = 26 and y = 30 mm, the values of gas temperature measured were slightly higher when using lines corresponding to transitions to $2s$ levels. This fact

was even more remarkable at the position y = 30 mm, closer to the end of the tube, and could be explained as a consequence of the entry of air into the plasma and the effect it has on W_W and W_R. Indeed, both of them depend on the composition of the gas feeding the discharge.

Theoretical determinations of C_W in Table II were made considering argon atoms as perturbers responsible for the van der Waals broadening of Ar I lines. In this way, reduced mass Ar-Ar and argon polarizability ($\mu_{Ar\text{-}Ar}$ = 19.97 and α_{Ar} = 16.54·10^{-25} cm^3) were considered. The presence of a portion of air in the plasma would modify the values of the van der Waals constant for the different lines, which mainly affect to determination of T_g from lines corresponding to transitions to *2s* levels, whose van der Waals contribution has a relative higher relevance. Also, C_R values would change, as they were originally calculated considering a proportion of a 100 % of argon perturber atoms in eq. (8).

In order to confirm this hypothesis, we have assumed some proportions of air in the plasma (20 and 40 % at positions y = 26 and y = 30 mm, respectively) for an estimate of the new T_{gas}. As a previous step, we had recalculated the theoretical dependence of W_W^{corr} and W_R^{corr} on T_{gas} assuming these air concentration proportions. For this purpose, we first determined the values of C_W' constants obtained considering air as perturber, so, using reduced mass Ar-Air and air polarizability ($\mu_{Ar\text{-}Air} \approx$ 16.81and $\alpha_{Air} \approx$ 2.10·10^{-23} cm^3) (see Table V). The new expression for the van der Waals broadening considering the air entry correction is given by

$$W_w^{corr}(T_g) = \chi_{Ar}\frac{C_W}{T_g^{0.7}} + \chi_{Air}\frac{C_W{}'}{T_g^{0.7}}\,(\text{nm}) \qquad (21)$$

being χ_{Ar} and χ_{Air} the molar fraction of argon and air in the discharge. For details the reader is referred to Yubero et al. [20].

A new expression for W_R^{corr} has been obtained from equation (8), considering the density of perturber atoms as equal to $N \approx \chi_{Ar} P/K_B T_g$, being χ_{Ar} the molar fraction of argon [9]. In this way:

$$W_R(T_g) = \chi_{Ar} \frac{C_R}{T_g} (\text{nm}) \tag{22}$$

being C_R the coefficient given in Table II.

Figures 12(a) and (b) show the dependence of $W_C(T_{gas})$ curve on the air concentration, for lines Ar I 750.39 m, and Ar I 842.46 nm, respectively. For the rest of lines, similar behaviors were found. For lines corresponding to $s_2 - p$ transitions, whose resonance broadenings are relatively high, the influence of the air on W_C was less important (see Fig. 12(a)). Conversely, broadenings of lines corresponding to $s_4 - p$ transitions are appreciably more affected.

Figure 13 shows the axial profile of T_g obtained considering these proportions of air. The agreement among the values of gas temperatures obtained with collisional broadening of the different lines is in this way improved for the two final positions, supporting our hypothesis.

3.2.2 Gas temperatures from OH(A-X) rotational band

OH (A-X) ro-vibrational band was also used for gas temperature determination, in order to validate the new methods we have presented. LIFBASE code developed by Luque and Crosley [35] was used for simulation of OH bands. At each axial position, LIFBASE was used to generate simulated spectra over a broad temperature range at coarse temperature increments of 20 K using a resolution of 0.065 nm. For each incremented temperature the residual is calculated as a value defined to be the sum of the differences between experimental and predicted intensity peak values across the entire spectral range. The

smallest residual of the full temperature range provided the rotational temperature according this code.

Figure 14 shows the values $T_{g,OH}$ derived from this band, and those obtained from Ar I 750.39 nm and Ar I 842.46 nm lines. Axial gas temperature profiles obtained from them were quite similar, within the experimental accuracy range of measurements. A very good agreement was also found when using the rest of Ar I lines considered here.

4. Final remarks.

In this paper we propose several (fourteen) new spectroscopic tools for determination of the gas temperature in non-thermal plasmas, based on the measurement of the collisional broadening of different (argon) atomic lines exhibiting a resonance broadening. Particularly, we used (fourteen) lines corresponding to transitions into both resonance levels s_2 and s_4 of the $3p^5 4s$ configuration of the Ar I system.

The method applies to argon plasmas with gas temperatures under 2000 K, and electron densities lower than 10^{15} cm^{-3}, because under these experimental conditions it has been shown that for these lines, the contributions of Doppler and Stark broadenings to the whole line profile are negligible when compared to resonance and van der Waals broadenings ones.

Also in this work, we have studied carefully the relative importance of all broadening mechanisms to the whole profile for these lines, under a broad range of experimental conditions (electron density and gas temperature). It has been shown that the van der Waals contribution should not be discarded for gas temperature determination, under any T_g condition.

Analytical expressions have been proposed for a straightforward determination of the gas temperature from the experimental collisional broadenings of these lines.

Similar methods using different atomic lines (helium, oxygen,…) could be also developed for plasmas operating in other gases.

Moreover, these new methods can be considered as good alternatives to those based on the measurement of rotational temperatures, as in the application of them, no assumptions on the degree of thermodynamic equilibrium existing in the plasma are needed.

Finally, the new methods we propose in this work (actually, nine of them) have been applied to gas temperature determination of an argon microwave jet open to the air. Values of the temperatures obtained using them, were consistent with each other. They were also compared to the rotational temperatures derived from the OH ro-vibrational bands, and a very good agreement was found. Results have also shown that the air entrance into this type of plasmas could affect gas temperature determination using these methods (in the experimental case presented here, this effect was observed at the end part of the plasma). We have indicated the way the method should be changed in order to take into account this air influence.

Aknowledgements

The authors thank the European Regional Development Funds program (EU-FEDER) and the MINECO (project MAT2016-79866-R) for financial support. Authors are also grateful to the *Física de Plasmas: Diagnosis, Modelos y Aplicaciones* (FQM 136) research group of Regional Government of Andalusia for technical and financial support.

REFERENCES

[1] T. Woedtke, H.R. Metelmann, and K.D. Weltmann, Clinical Plasma Medicine: State and Perspectives of in Vivo Application of Cold Atmospheric Plasma, Contrib. Plasma Phys. 54 (2014), pp. 104-11.

[2] J. Gay-Mimbrera, M.C. García, B. Isla-Tejera, A. Rodero-Serrano, A. Velez Garcia-Nieto, J. Ruano, Clinical and Biological Principles of Cold Atmospheric Plasma Application in Skin Cancer, Adv. Ther. 33 (2016), pp. 894-909.

[3] T. Woedtke, S. Reuter, K. Masur, K.D. Weltmann, Plasmas for medicine, Physics Reports 530 (2013) pp. 291–320.

[4] G. Isbary, J.L. Zimmermann, T. Shimizu, Y.F. Li, G.E. Morfill, H.M. Thomas, B. Steffes, J. Heinlin, S. Karrer, W. Stolz, Non-thermal plasma—More than five years of clinical experience, Clinical Plasma Medicine 1 (2013) pp. 19–23.

[5] M G Kong, G Kroesen, G Morfill, T Nosenko, T Shimizu, J van Dijk and J L Zimmermann, Plasma medicine: an introductory review, New Journal of Physics 11 (2009) 115012 (35pp).

[6] X.M. Zhu, W.C. Chen and Y.K. Pu, Gas temperature, electron density and electron temperature measurement in a microwave excited microplasma, J. Phys. D: Appl. Phys. 41 (2008) 105212 (6pp).

[7] Q. Wang, I. Koleva, V.M. Donnelly and D.J. Economou, Spatially resolved diagnostics of an atmospheric pressure direct current helium microplasma, J. Phys. D: Appl. Phys. 38 (2005) 1690-1697.

[8] M.H. Abdallah and J.M. Mermet, The Behavior of Nitrogen Excited in an Inductively Coupled Argon Plasma, J. Quant. Spectrosc. Radiat. Transfer. 19 (1978) 83-91.

[9] C.O. Laux, T.G. Spence, C.H. Kruger and R.N. Zare, Optical diagnostics of atmospheric pressure air plasmas, Plasma Sources Sci. Technol. 12 (2003) 125-138.

[10] U. Fantz, Emission spectroscopy of molecular low pressure plasmas, Contrib. Plasma Phys. 44 (5-6), 508-515 (2004).

[11] M. Mora, M.C. García, C. Jiménez-Sanchidrián and F.J. Romero-Salguero, Transformation of light paraffins in a microwave-induced plasma-based reactor at reduced pressure, Int. J. Hydrogen Energy 35 (2010) 4111-4122.

[12] F. Iza and J.A. Hopwood, Rotational, vibrational, and excitation temperatures of a microwave-frequency microplasma, IEEE Trans. Plasma Sci. 32 (2) (2004) 498-504.

[13] G. Lombardi, F. Benedic, F. Mohasseb, K. Hassouni and A. Gicquel, Determination of gas temperature and C-2 absolute density in Ar/H-2/CH4 microwave discharges used for nanocrystalline diamond deposition from the C-2 Mulliken system, Plasma Sources Sci. Technol. 13 (2004) 375-386.

[14] P. Bruggeman, D.C. Schram, M.G. Kong and C. Leys, Is the Rotational Temperature of OH(A-X) for Discharges in and in Contact with Liquids a Good Diagnostic for Determining the Gas Temperature?, Plasma Process. Polym. 6 (2009), 751-762.

[15] J. Henriques, E. Tatarova and C.M. Ferreira, Microwave N-2-Ar plasma torch. I. Modeling, J. Appl. Phys. 109, (2011) 023301.

[16] P. Bruggeman, D.C. Schram, M.A. González, R. Rego, M.G. Kong and C. Leys, Characterization of a direct dc-excited discharge in water by optical emission spectroscopy, Plasma Sources Sci. Technol. 18 (2009) 025017 (13 pp)

[17] P. Bruggeman, T. Verreycken, M.A. González, J.L. Walsh, M.G. Kong, C. Leys and D.C. Schram, Optical emission spectroscopy as a diagnostic for plasmas in liquids: opportunities and pitfalls, J. Phys. D: Appl. Phys. 43 (2010) 124005 (8pp).

[18] A.V. Pipa, Yu.Z. Ionikh, V.M. Chekishev, M. Dünnbier, and S. Reuter, Resonance broadening of argon lines in a micro-scaled atmospheric pressure plasma jet (argon μ APPJ), Appl. Phys. Lett. 106 (2015) 244104 (5pp).

[19] M. Christova, E. Castaños-Martínez, M.D. Calzada, Y. Kabouzi, J.M. Luque and M. Moisan, Electron density and gas temperature from line broadening in an argon surface-wave-sustained discharge at atmospheric pressure, Appl. Spectrosc. 58 (2004) 1032-1037.

[20] M. Christova, V. Gagov and I. Koleva, Analysis of the profiles of the argon 696.5 nm spectral line excited in non-stationary wave-guided discharges, Spectrochim. Acta B 55 (2000) 815-822.

[21] C. Yubero, M.S. Dimitrijevic, M.C. García and M.D. Calzada, Using the van der Waals broadening of the spectral atomic lines to measure the gas temperature of an argon microwave plasma at atmospheric pressure, Spectrochim. Acta B 62 (2007) 169-176.

[22] J. Muñoz, M.S. Dimitrijevic, C. Yubero and M.D. Calzada, Using the van der Waals broadening of spectral atomic lines to measure the gas temperature of an argon-helium microwave plasma at atmospheric pressure, Spectrochim. Acta B 64 (2009) 167-172.

[23] C. Yubero, A. Rodero, M.S. Dimitrijevic, A. Gamero, M.C. García, Gas temperature determination in an argon non-thermal plasma at atmospheric pressure from broadenings of atomic emission lines, Spectrochim. Acta B 129 (2017) 14-20.

[24] N. Allard and J. Kielkopf. The effect of neutral non resonant collisions on atomic spectral lines Rev. Mod. Phys., 54 (1982), pp. 1103–1182.

[25] A.W. Ali and H.R. Giem, Theory of Resonance Broadening of Spectral Lines by Atom-Atom Impacts, Phys. Rev. 140 (4A) (1965) 1044-1049.

[26] A. W. Ali and H. R. Griem. Theory of Resonance Broadening of Spectral Lines by Atom-Atom Impacts (ERRATA), Phys. Rev. 144 (1966) 366.

[27] A. Y. Nikiforov, C. Leys, M. A. Gonzalez and J. L. Walsh, Electron density measurement in atmospheric pressure plasma jets: Stark broadening of hydrogenated and non-hydrogenated lines, Plasma Sources Sci. Technol. 24 (2015) 034001 (18pp).

[28] N. Konjevic, Plasma broadening and shifting of non-hydrogenic spectral lines: present status and applications, Physics Reports 316 (1999) pp. 339-401.

[29] N. Konjevic and W. L. Wiese, Experimental Stark Widths and Shifts for Spectral Lines of Neutral and Ionized Atoms (A Critical Review of Selected Data for the Period 1983 Through 1988), J. Phys. Chem. Ref. Data, 19 (1990) pp. 1307-1385.

[30] N. Konjevic, A. Lesage, J. R. Fuhr and W. L. Wiese, Experimental Stark Widths and Shifts for Spectral Lines of Neutral and Ionized Atoms (A Critical Review of Selected Data for the Period 1989 Through 2000), J. Phys. Chem. Ref. Data, 31(2002) pp. 819-927.

[31] H. R. Griem: 1974, Spectral Line Broadening by Plasmas, New York, Academic Press.

[32] A. Kramida, Yu. Ralchenko and J. Reader, NIST ASD Team (20l6). *NIST Atomic Spectra Database* (version 5.4), [Online]. Available: http://physics.nist.gov/asd [Thu Jan 12 2017]. National Institute of Standards and Technology, Gaithersburg, MD.

[33] M. Moisan and J. Pelletier: 1992, Microwave excited plasmas, Plasma Technology, Elsevier, Amsterdan, (Chap. 3).

[34] S. Hofmann, A. F. H. van Gessel, T. Verreycken and P. Bruggeman, Power dissipation, gas temperatures and electron densities of cold atmospheric pressure helium and argon RF plasma jets, Plasma Sources Sci. Technol. 20 (2011) 065010 (12pp).

[35] J. Luque and D. R. Crosley, LIFBASE: Database and spectral simulation program (version 1.5), SRI International Report MP 99 (1999) 009.

FIGURE CAPTIONS

Fig.1. Contribution of each collisional mechanism to W_C, as a function of T_g in the case of resonance and van der Waals broadenings, and as a function of n_e in the case of the Stark broadening (T_e = 10,000 K).

Fig. 2. Dependence of W_C on T_g for different values of electron densities (**(a)** for line Ar I 750.39 nm; **(b)** for line Ar I 842.46 nm).

Fig. 3. W_C values obtained with and without considering the van der Waals contribution (**(a)** for line Ar I 750.39 nm and **(b)** for line Ar I 842.46 nm).

Fig. 4. W_V values obtained considering and not considering the Doppler contribution (**(a)** for line Ar I 750.39 nm and **(b)** for line ArI 842.46 nm).

Fig. 5. T_g (W_C) curves **(a)** for line Ar I 750.39 nm and **(b)** for line Ar I 842 nm.

Fig. 6. T_g (W_C) curves for all Ar I lines considered in this work.

Fig. 7. Experimental set-up.

Fig. 8. Characteristic OES spectrum emitted by the discharge.

Fig. 9. Averaged values of W_V measured for the nine resonance lines detected, for different *y* positions in the plasma.

Fig. 10. Collisional broadening measured from W_V for the Ar I lines studied, for different *y* positions in the plasma.

Fig. 11. Values of T_g measured from different Ar I lines.

Fig. 12. Dependence of W_C (T_{gas}) curve on the air concentration, for lines (a) Ar I 750.39 m, and (b) Ar I 842.46 nm.

Fig. 13. Values of T_g obtained considering 20 % and 40 % of air at y = 26 mm and y = 30 mm, respectively.

Fig. 14. Values $T_{g,OH}$ derived from OH (A-X) ro-vibrational band, and those obtained from Ar I 750.39 nm and Ar I 842.46 nm lines.

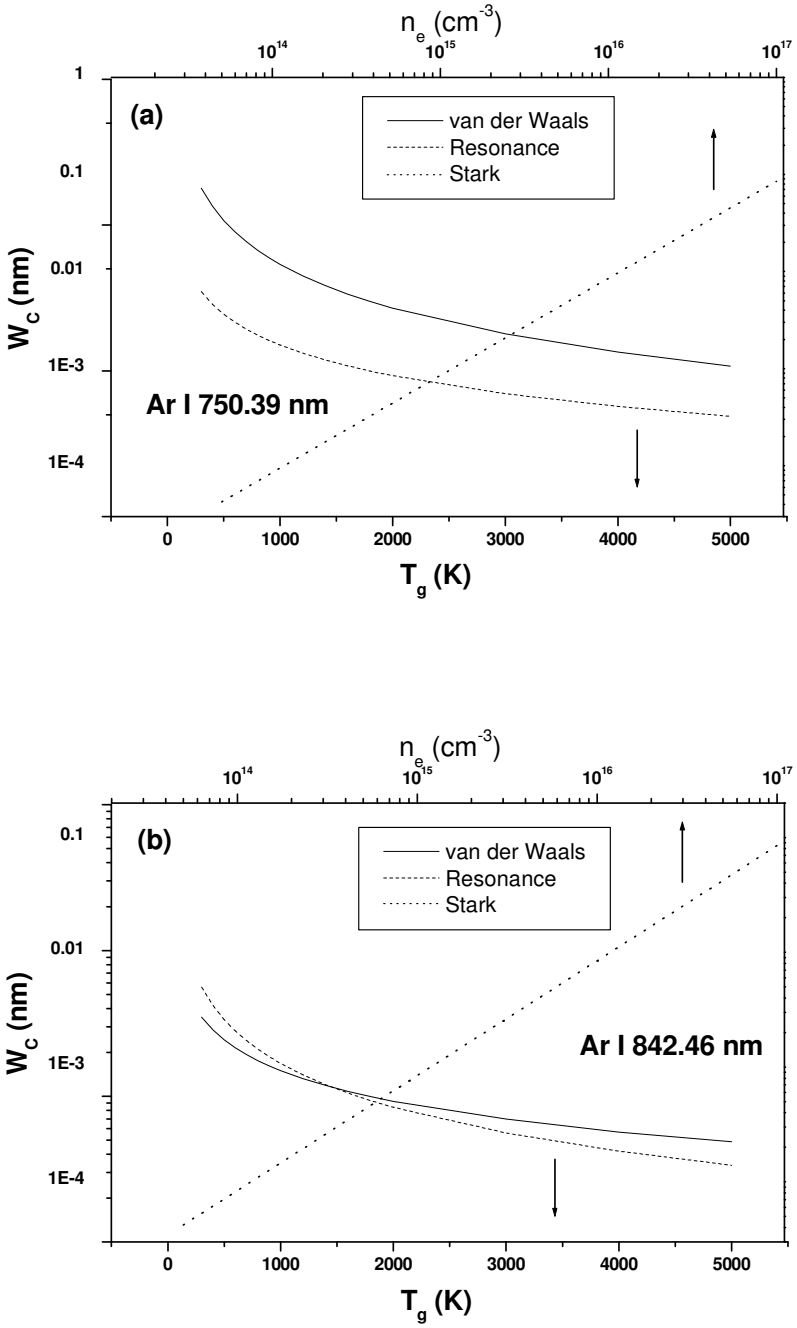

Fig. 1. Contribution of each collisional mechanism to W_C, as a function of T_g in the case of resonance and van der Waals broadenings, and as a function of n_e in the case of the Stark broadening (T_e = 10,000 K).

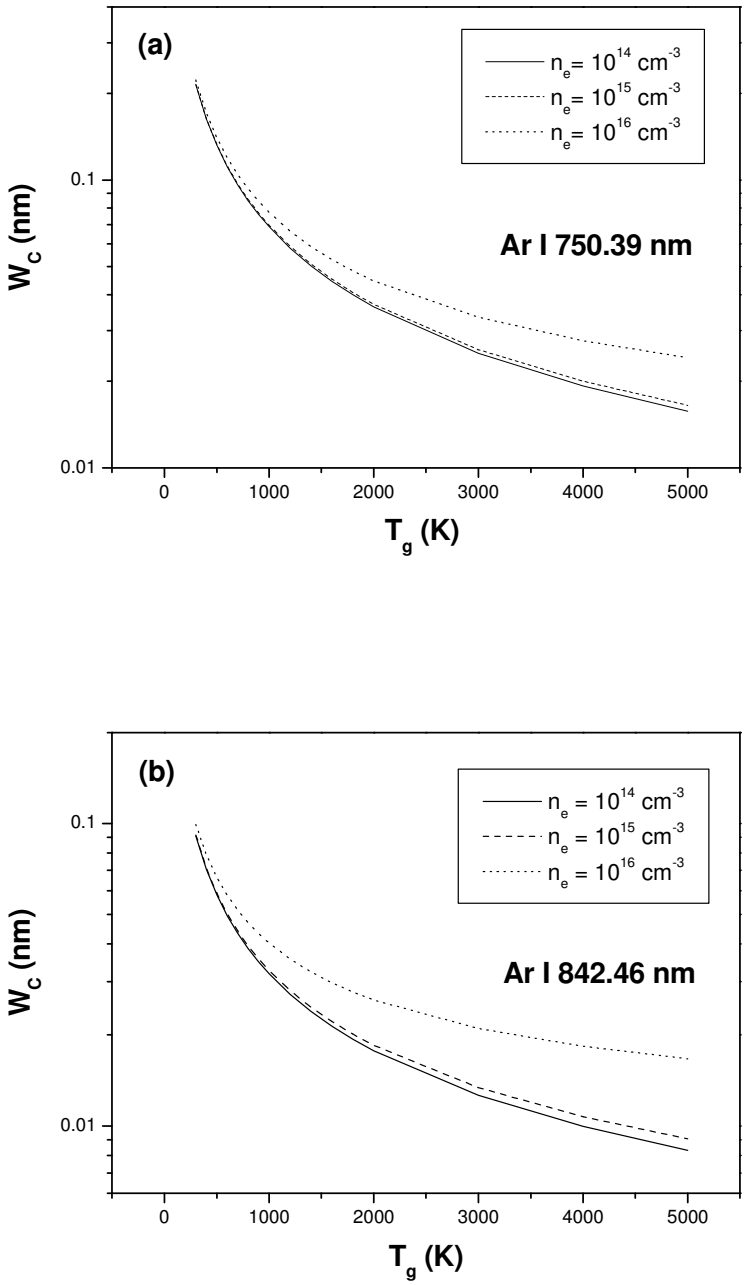

Fig. 2. Dependence of W_C on T_g for different values of electron densities (**(a)** for line Ar I 750.39 nm; **(b)** for line Ar I 842.46 nm).

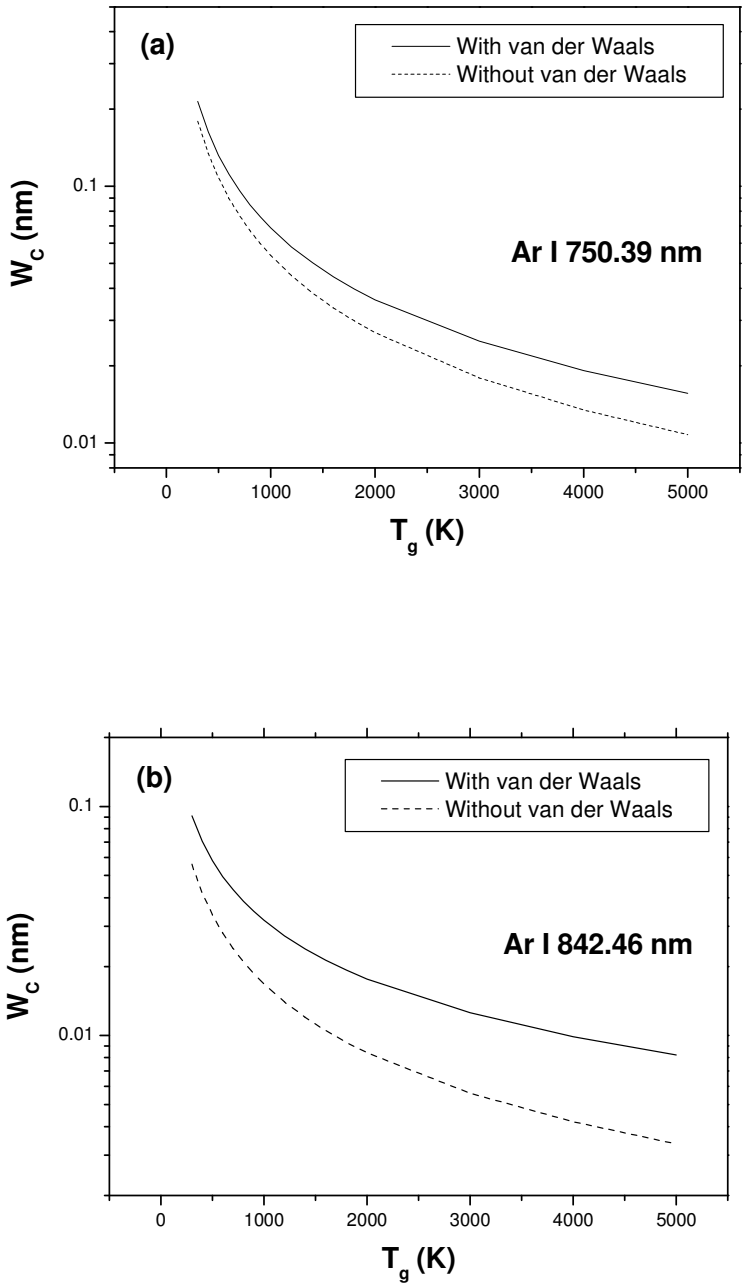

Fig. 3. W_C values obtained with and without van der Waals contribution ((**a**) for line Ar I 750.39 nm and **(b)** for line Ar I 842.46 nm).

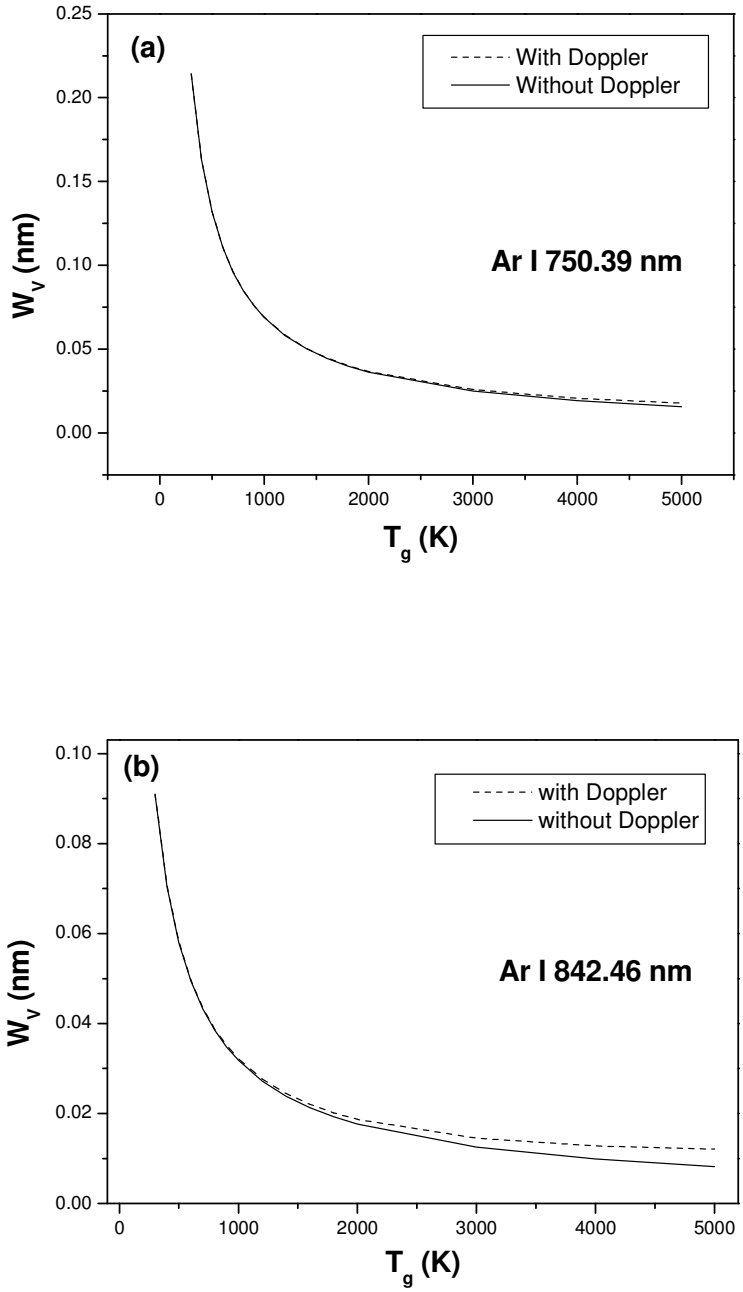

Fig. 4. W_V values obtained considering and not considering the Doppler contribution ((**a**) for line Ar I 750.39 nm and **(b)** for line ArI 842.46 nm).

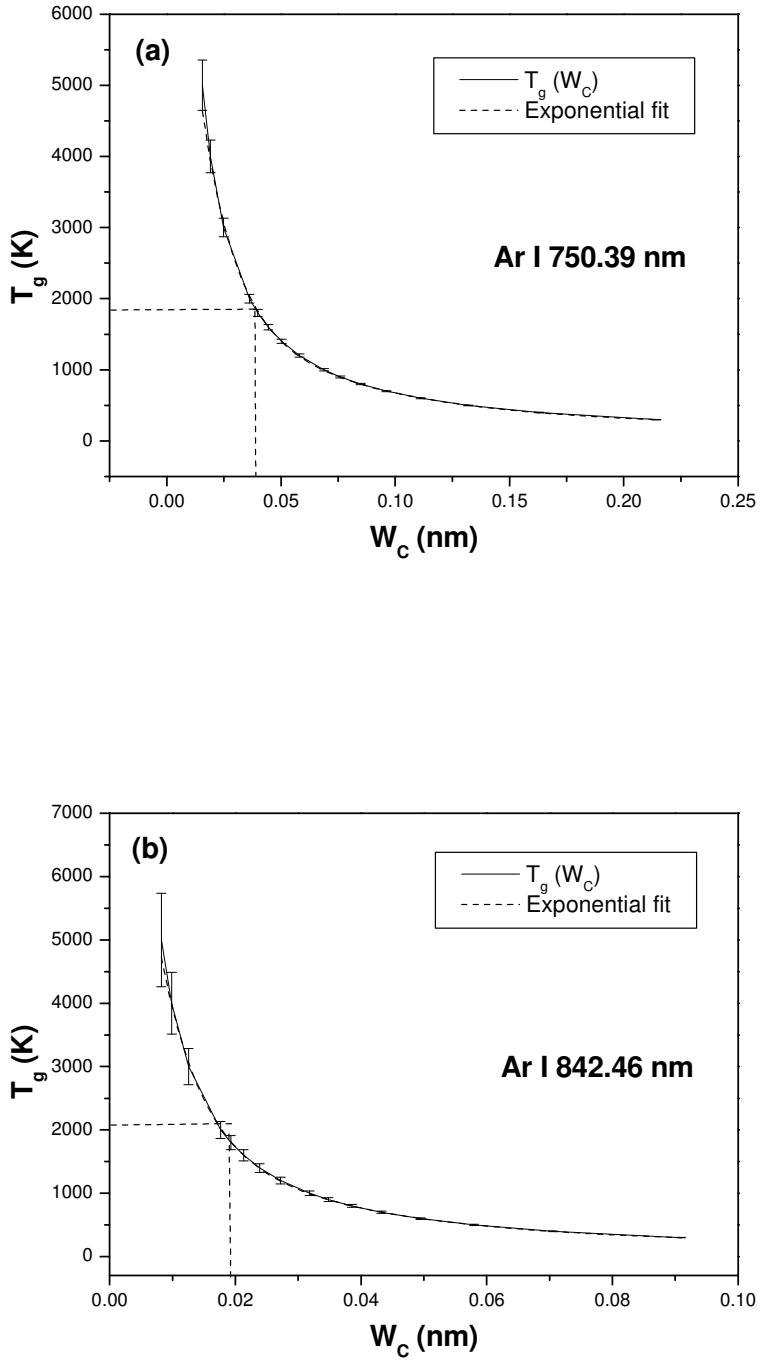

Fig. 5. T_g (W_C) curves **(a)** for line Ar I 750.39 nm and **(b)** for line Ar I 842 nm.

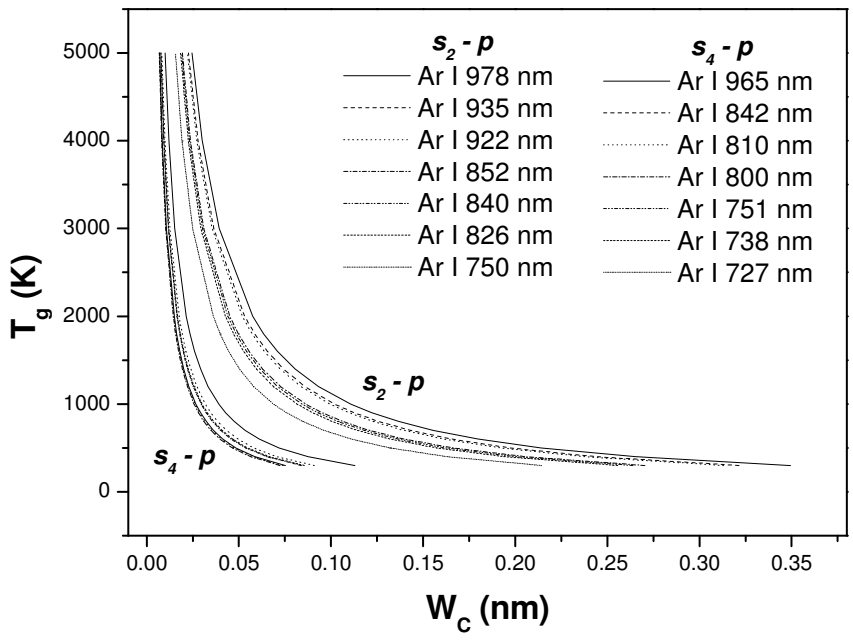

Fig. 6. T_g (W_C) curves for all Ar I lines considered in this work.

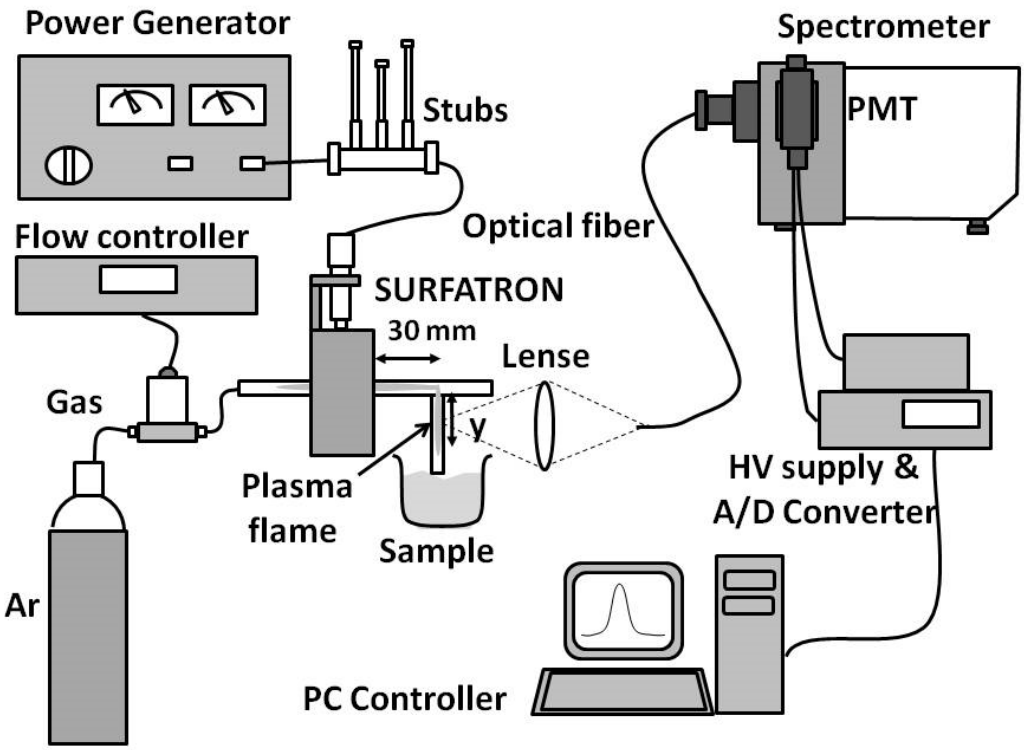

Fig. 7. Experimental set-up.

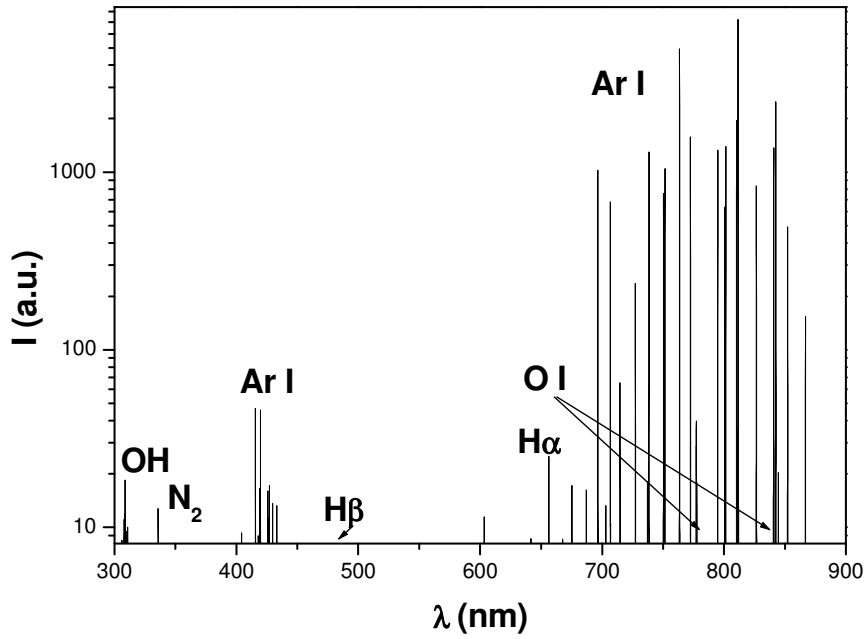

Fig. 8. Characteristic OES spectrum emitted by the discharge.

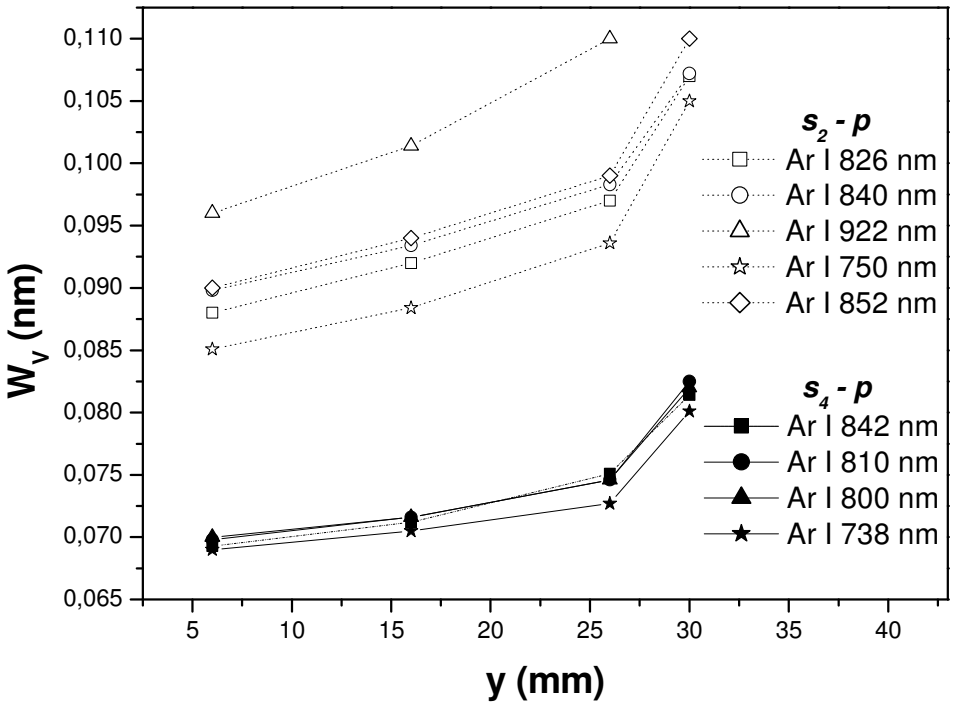

Fig. 9. Averaged values of W_V measured for the nine resonance lines detected, for different y positions in the plasma.

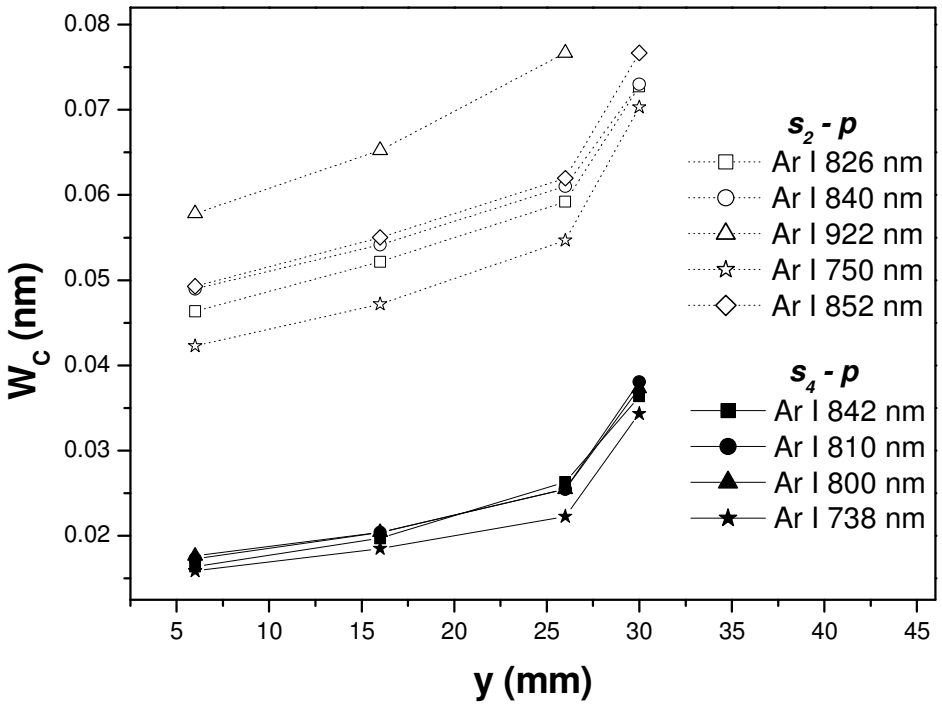

Fig. 10. Collisional broadening measured from W_V for the Ar I lines studied, for different *y* positions in the plasma.

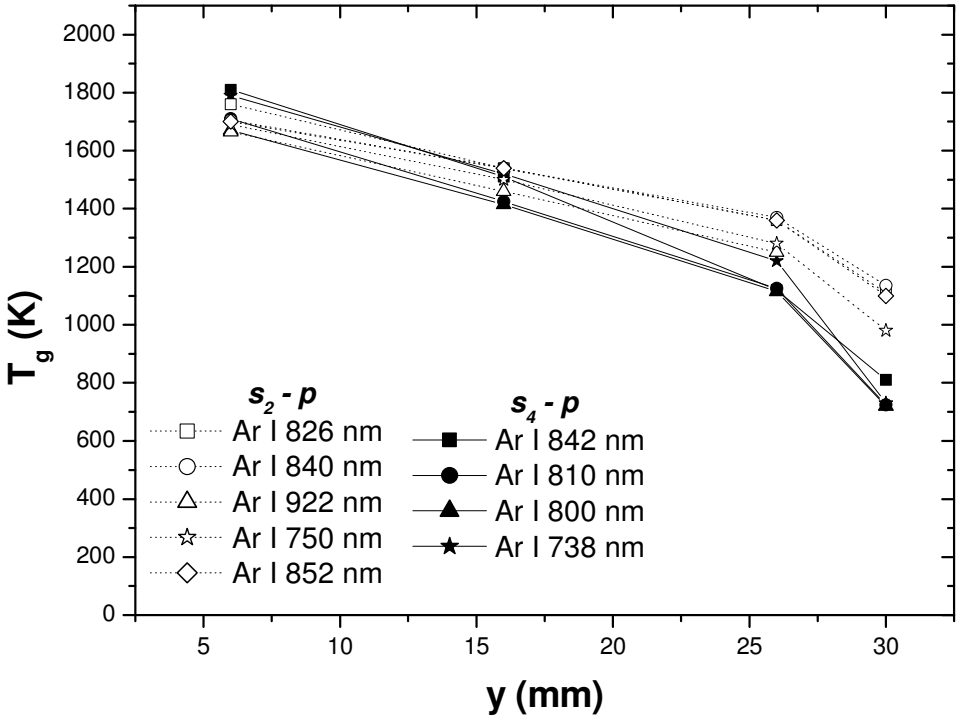

Fig. 11. Values of T_g measured from different Ar I lines.

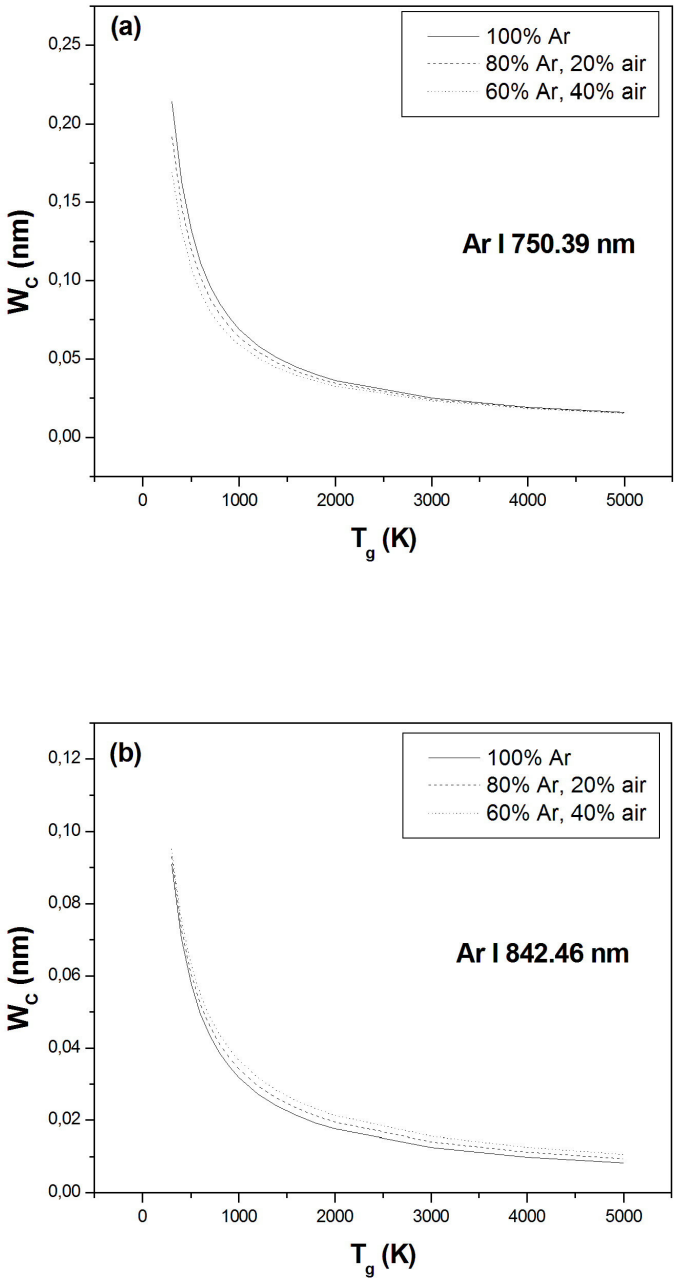

Fig. 12. Dependence of W_C (T_{gas}) curve on the air concentration, for lines **(a)** Ar I 750.39 m, and **(b)** Ar I 842.46 nm.

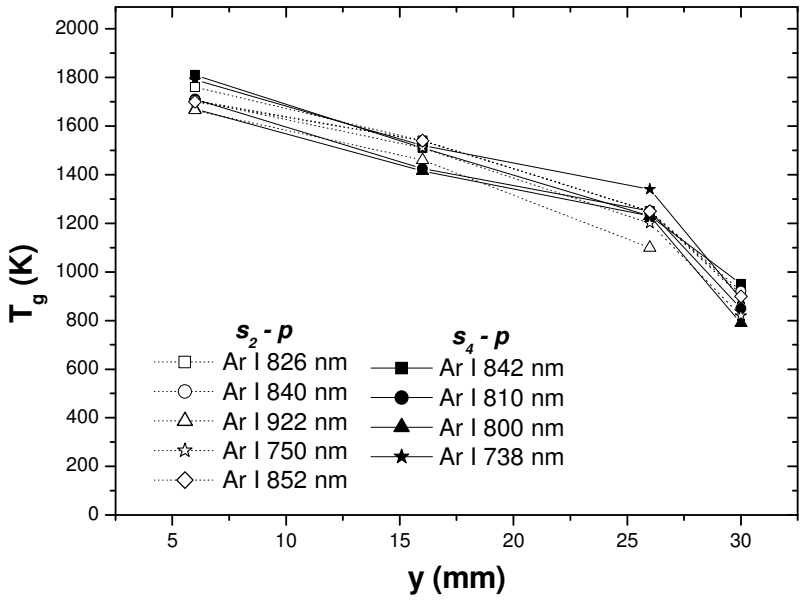

Fig. 13. Values of T_g obtained considering 20 % and 40 % of air at y = 26 mm and y = 30 mm, respectively.

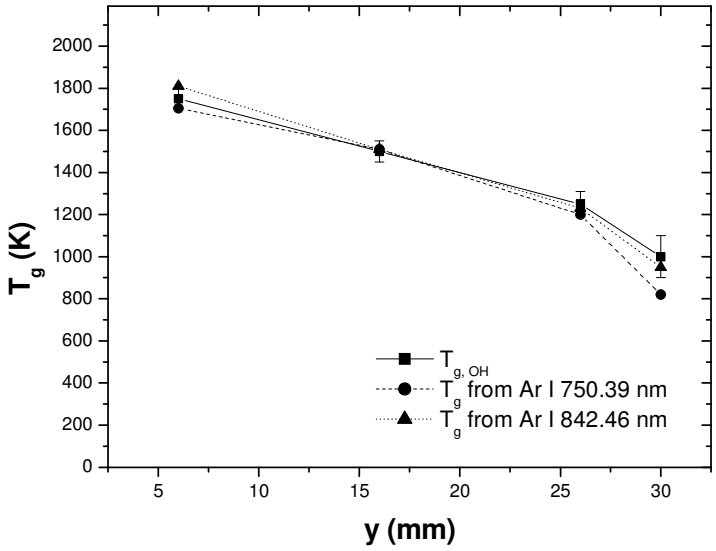

Fig. 14. Values $T_{g,OH}$ derived from OH (A-X) ro-vibrational band, and those obtained from Ar I 750.39 nm and Ar I 842.46 nm lines.

Table I. Some characteristics parameters of the argon atomic lines corresponding to transitions into the resonance levels s_2 and s_4 of the $3p^5 4s$ configuration of argon atomic system, used in this work [32].

Ar I lines	f	E_l - E_u (cm^3)	g_l - g_u
		s_2 - p	
978.45 nm	3.52e-02	95 399.8276 - 105 617.2700	3 - 5
935.42 nm	1.39e-02	95 399.8276 - 106 087.2598	3 - 3
922.45 nm	1.07e-01	95 399.8276 - 106 237.5518	3 - 5
852.14 nm	1.51e-01	95 399.8276 - 107 131.7086	3 - 3
840.82 nm	3.94e-01	95 399.8276 - 107 289.7001	3 - 5
826.45 nm	1.57e-01	95 399.8276 - 107 496.4166	3 - 3
750.39 nm	1.25e-01	95 399.8276 - 108 722.6194	3 - 1
		s_4- p	
965.77 nm	7.60e-02	93 750.5978 - 104 102.0990	3 - 3
842.46 nm	3.81e-01	93 750.5978 - 105 617.2700	3 - 5
810. 37 nm	2.5e-01	93 750.5978 - 106 087.2598	3 - 3
800.62 nm	7.85e-02	93 750.5978 - 106 237.5518	3 - 5
751.46 nm*	1.14e-01	93 750.5978 - 107 054.2720	3 - 1
738.40 nm	1.15e-01	93 750.5978 - 107 289.7001	3 - 5
727.29 nm*	1.45e-02	93 750.5978 - 107 496.4166	3 - 3

Table II. Constants for van der Waals and resonance broadenings and Stark parameters (n_e=10^{16} cm^{-3}, T_e=10,000 K) for the different Ar I lines used.

Ar I lines	C_W	C_R	w_e (nm)
		s_2 - p	
978.45 nm	2.417	91.431	-
935.42 nm	2.318	83.566	-
922.45 nm	2.289	81.265	0.0145 [30]
852.14 nm	2.126	69.349	0.0102 [30]
840.82 nm	2.100	67.519	0.0111 [31]
826.45 nm	2.067	65.231	0.0092 [30]
750.39 nm	1.893	53.776	0.0085 [30]
		s_4 - p	
965.77 nm	2.136	22.080	-
842.46 nm	1.891	16.802	0.0084 [31]
810. 37 nm	1.825	15.546	0.011 [31]
800.62 nm	1.805	15.174	0.0087 [30]
751.46 nm[sol]	1.706	13.367	0.0074 [30]
738.40 nm	1.680	12.907	0.0071 [30]
727.29 nm[sol]	1.657	12.522	0.0096 [30]

TABLE III. Analytical functions from curves in Fig. 6 allowing a straightforward determination of the gas temperature from W_C.

Line	Analytical function
	$s_2 - p$
Ar I 978.45	$T_g(W_c) = 0.296 + 13.68\exp\left(-\frac{W_c}{0.0143}\right) + 3.073\exp\left(-\frac{W_c}{0.0758}\right)(\times 10^3\,K)$
Ar I 935.42	$T_g(W_c) = 0.296 + 13.75\exp\left(-\frac{W_c}{0.0132}\right) + 3.080\exp\left(-\frac{W_c}{0.0698}\right)(\times 10^3\,K)$
Ar I 922.45	$T_g(W_c) = 0.296 + 13.77\exp\left(-\frac{W_c}{0.0129}\right) + 3.082\exp\left(-\frac{W_c}{0.0680}\right)(\times 10^3\,K)$
ArI 852.14	$T_g(W_c) = 0.295 + 13.92\exp\left(-\frac{W_c}{0.0113}\right) + 3.095\exp\left(-\frac{W_c}{0.0588}\right)(\times 10^3\,K)$
ArI 840.82	$T_g(W_c) = 0.295 + 13.94\exp\left(-\frac{W_c}{0.0109}\right) + 3.098\exp\left(-\frac{W_c}{0.0574}\right)(\times 10^3\,K)$
ArI 826.45	$T_g(W_c) = 0.295 + 13.97\exp\left(-\frac{W_c}{0.0106}\right) + 3.101\exp\left(-\frac{W_c}{0.0556}\right)(\times 10^3\,K)$
ArI 750.39	$T_g(W_c) = 0.294 + 14.16\exp\left(-\frac{W_c}{0.0089}\right) + 3.118\exp\left(-\frac{W_c}{0.0468}\right)(\times 10^3\,K)$
	$s_4 - p$
ArI 965.77	$T_g(W_c) = 0.283 + 16.63\exp\left(-\frac{W_c}{0.0052}\right) + 3.366\exp\left(-\frac{W_c}{0.0254}\right)(\times 10^3\,K)$
ArI 842.46	$T_g(W_c) = 0.281 + 17.08\exp\left(-\frac{W_c}{0.0042}\right) + 3.414\exp\left(-\frac{W_c}{0.0205}\right)(\times 10^3\,K)$
ArI 810.37	$T_g(W_c) = 0.280 + 17.21\exp\left(-\frac{W_c}{0.0040}\right) + 3.429\exp\left(-\frac{W_c}{0.0193}\right)(\times 10^3\,K)$
ArI 800.62	$T_g(W_c) = 0.280 + 17.25\exp\left(-\frac{W_c}{0.0039}\right) + 3.433\exp\left(-\frac{W_c}{0.0190}\right)(\times 10^3\,K)$
ArI 751.46	$T_g(W_c) = 0.279 + 17.53\exp\left(-\frac{W_c}{0.0035}\right) + 3.464\exp\left(-\frac{W_c}{0.0171}\right)(\times 10^3\,K)$

ArI 738.40	$T_g(W_c) = 0.279 + 17.53\exp\left(-\frac{W_c}{0.0035}\right) + 3.464\exp\left(-\frac{W_c}{0.0168}\right)(\times 10^3\,K)$
ArI 727.29	$T_g(W_c) = 0.279 + 17.60\exp\left(-\frac{W_c}{0.0034}\right) + 3.473\exp\left(-\frac{W_c}{0.0164}\right)(\times 10^3\,K)$

TABLE IV. Values of FWHM of instrumental funtion for wavelengths corresponding to Ar I used in this work (slit widht of 77 μm).

Ar I lines	W_I (nm)
922.45 nm	0.05725
852.14 nm	0.05870
842.46 nm	0.05884
840.82 nm	0.05888
826.45 nm	0.05913
810. 37 nm	0.05941
800.62 nm	0.05958
750.39 nm	0.06036
738.40 nm	0.06054

Table V. Constants for van der Waals broadening for the different Ar I lines used, considering air as perturber.

Ar I lines	C_W'
$s_2 - p$	
978.45 nm	7.034
935.42 nm	6.745
922.45 nm	6.660
852.14 nm	6.186
840.82 nm	6.110
826.45 nm	6.014
750.39 nm	5.508
$s_4 - p$	
965.77 nm	6.216
842.46 nm	5.502
810. 37 nm	5.312
800.62 nm	5.254
751.46 nm^{sol}	4.964
738.40 nm	4.888
727.29 nm^{sol}	4.823

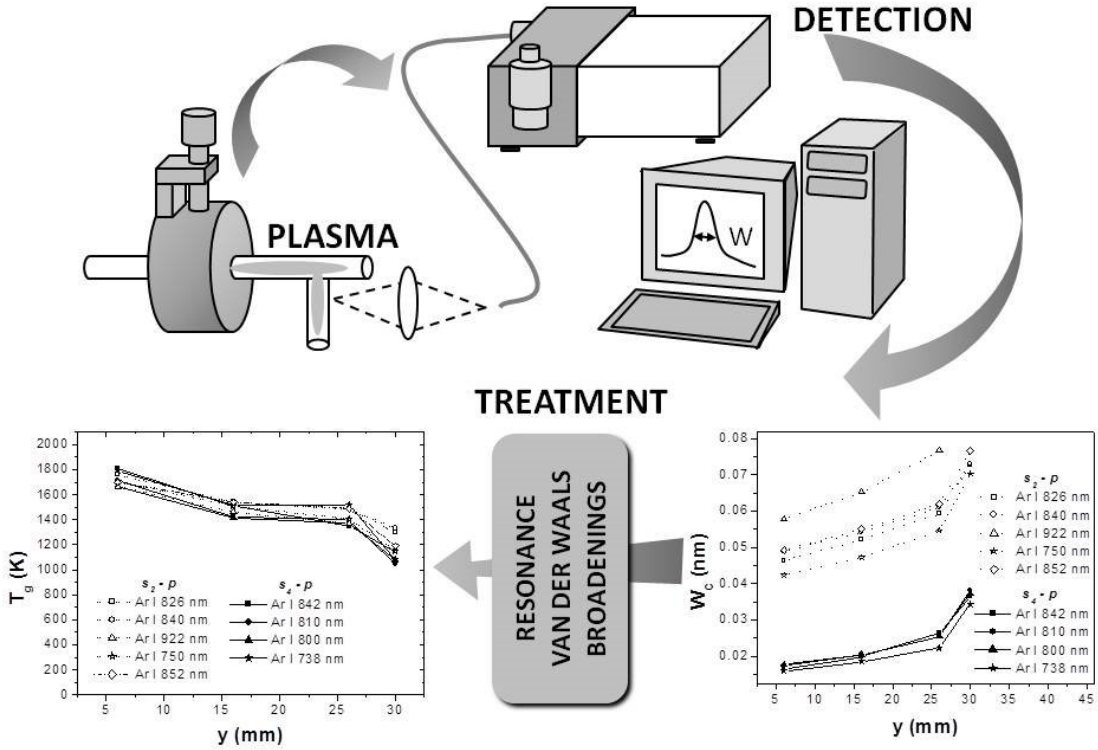
DETECTION
PLASMA
W
TREATMENT
RESONANCE
VAN DER WAALS
BROADENINGS
T_g (K)
y (mm)
s_2 - p
Ar I 826 nm
Ar I 840 nm
Ar I 922 nm
Ar I 750 nm
Ar I 852 nm
s_4 - p
Ar I 842 nm
Ar I 810 nm
Ar I 800 nm
Ar I 738 nm
W_c (nm)
y (mm)

HIGHLIGHTS

- A new method to measure the gas temperature in non-thermal plasmas from the collisional broadening of some argon atomic lines is presented.
- These lines correspond to transitions into both resonance levels s_2 and s_4 of the $3p^5 4s$ configuration of the Ar I system.
- For these lines, the van der Waals contribution should not be ever discarded in gas temperature determination.
- Analytic expressions allowing straightforward determination of the gas temperature from the collisional broadening are given.
- Results are in good agreement with those obtained using other diagnostic methods.
- No assumptions on the degree of equilibrium existing in the plasma are needed**.**